Proceedings of the 1998 IEEE
International Conference on Robotics & Automation
Leuven, Belgium • May 1998

Robust Path-following Control with Exponential Stability for Mobile Robots

L.E. Aguilar M. P. Souères M. Courdesses S. Fleury

L.A.A.S. - C.N.R.S.
7 Av. du Colonel Roche
31077 Toulouse Cedex 4 - France
e-mail: {luis, soueres, courdess, sara}@laas.fr

Abstract

In this paper, we present a new method allowing to determine a path following controller for a nonholonomic mobile robot, robust with respect to position and orientation errors. We consider successively the kinematic model of a unicycle and a dynamic extension. The control design is based on a change of variables allowing to define a set of n decoupled auxiliary variables. The exponential convergence of the state variables is deduced from the convergence of the auxiliary variables. We prove the control robustness by showing that, when the state variables measurement is noisy, the representative point of the system converges towards a compact attractive domain centered at the equilibrium point. As the auxiliary variables are decoupled, the computation of this attractive domain is done in a very simple and accurate way. The determination of such a domain can be used to determine a security margin to avoid obstacles during the path following process.

1 Introduction

Due to both its richness and hardness, the problem of controlling nonholonomic mobile robots has motivated a large number of research works involving various techniques of automatic control. However, in most cases, the control problem is stated in terms of stabilizing a simple mathematical model, and the state variables are supposed to be exactly known at each time. Whereas such a model allows to consider the main feature of wheeled robot, namely the nonholonomic rolling without slipping constraint, it does not take into account several intrinsic characteristics of the system such as the actual vehicle dynamics, the inertia and power limit of actuators, the localization errors, etc. For this reason, the question of designing robust controllers, with respect to measure and model errors, appears to be central in mobile robotics today. In this paper, we focus on the design of robust controllers with respect to localization errors. A first result in this direction was obtained by Hamel [4] who considered the problem of parking a robot between two walls. In [5], a robust path following control with respect to localization errors is proposed. The method is based on Lyapunov's direct technique and the design of a sliding variable defined as a linear combination of the state variables. This result has been improved in [1] by introducing a variable structure control. We present here a new method allowing to determine a path following controller robust with respect to localization errors. We consider successively the kinematic model of a unicycle and a dynamic extension. The control design is based on a change of variables allowing to define a set of n decoupled auxiliary variables. Drawing our inspiration from linear control techniques, we determine a controller ensuring the exponential convergence of each of these new variables to zero. The exponential convergence of the state variable is deduced from this result. When the state variables measurement is noisy, we show that the representative point of the system converges towards a compact attractive domain centered at the equilibrium point. As the auxiliary variables are decoupled, the computation of this attractive domain is done in a very simple and accurate way. The determination of such a domain can be used to determine a security margin to avoid obstacles when the system has reached its steady state. In the first section we present the kinematic model of the robot and we state the path following problem. The stabilizing controller is determined in section 2. The control robustness is proven in section 3. In section 4, we show succinctly how the method can be applied to stabilize a more realistic extended model. Finally, experimental results are described in the last section.

2 Problem statement

A configuration of the robot is represented by a vector $P_c = (x_c, y_c, \theta_c)$ where (x_c, y_c) are the coordinates of a reference point c with respect to the world frame $\mathcal{W}$; and the angle $\theta_c \in S^1$ represents the direction of the vehicle with

0-7803-4300-x-5/98 $10.00 © 1998 IEEE

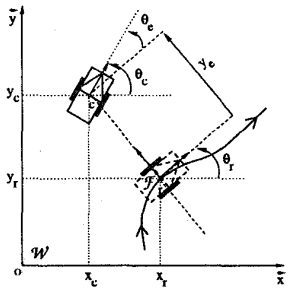

Figure 1: Description of the Path Following Problem

respect to the x-axis. The robot kinematics is described by :

$$\dot{P}_c = \begin{pmatrix} \dot{x}_c \\ \dot{y}_c \\ \dot{\theta}_c \end{pmatrix} = \begin{pmatrix} v_c \cos\theta_c \\ v_c \sin\theta_c \\ \omega_c \end{pmatrix} \quad (1)$$

where $v_c(t), \omega_c(t)$ represent respectively the linear and the angular velocities of the vehicle.

The path-following problem consists in determining the angular velocity ω_c allowing the robot to follow the reference path, regardless of its linear velocity v_c which is just supposed to be nonzero[1]. We use the modeling given in [6] to represent the problem (see figure 1). The orthogonal projection of the robot position on the reference path defines a moving frame $\mathcal{F}$ oriented in the direction to follow. Let (x_r, y_r) be the coordinates of the origin of $\mathcal{F}$ and θ_r the orientation of the x_r-axis with respect to $\mathcal{W}$. $\mathcal{F}$ can be interpreted as the frame of a kinematically equivalent fictitious robot whose configuration is $P_r = (x_r, y_r, \theta_r)^T$. With respect to this moving frame, the configuration error $P_e = P_c - P_r$ expresses as :

$$P_e = \begin{pmatrix} x_e \\ y_e \\ \theta_e \end{pmatrix} = \begin{pmatrix} \cos\theta_r(x_c - x_r) + \sin\theta_r(y_c - y_r) \\ -\sin\theta_r(x_c - x_r) + \cos\theta_r(y_c - y_r) \\ \theta_c - \theta_r \end{pmatrix} \quad (2)$$

Taking the time derivative, we get :

$$\dot{P}_e = \begin{pmatrix} \dot{x}_e \\ \dot{y}_e \\ \dot{\theta}_e \end{pmatrix} = \begin{pmatrix} \omega_r\, y_e - v_r + v_c \cos\theta_e \\ -\omega_r\, x_e + v_c \sin\theta_e \\ \omega_c - \omega_r \end{pmatrix} \quad (3)$$

By definition of the orthogonal projection x_e and $\dot{x}_e$ remain equal to zero as the robot moves. Therefore, from the first equation of (3) we have :

$$v_r = y_e\, w_r + v_c \cos\theta_e \quad (4)$$

Under the hypothesis that the reference path curvature $\chi_r = \frac{\omega_r}{v_r}$ is continuous and bounded, this last expression can be rewritten as :

$$v_r = \left(\frac{\cos(\theta_e)}{1 - \chi_r y_e}\right) v_c \quad (5)$$

under the constraint[2]: $(1 - \chi_r y_e) > 0$

As the linear velocity of the robot is not controlled, it suffices to consider the following reduced system made of the last two lines of (3) :

$$\begin{aligned} \dot{y}_e &= v_c \sin\theta_e \\ \dot{\theta}_e &= \omega_e \end{aligned} \quad (6)$$

where

$$\omega_e = \omega_c - \omega_r = \omega_c - \left[\chi_r \left(\frac{\cos(\theta_e)}{1 - \chi_r y_e}\right)\right] v_c \quad (7)$$

With this modeling, the path following problem has been turned into the problem of determining a closed-loop control ω_e to stabilize the system (6) to the origin $(y_e, \theta_e) = (0, 0)$.

NB : *In the sequel, $\sigma(v_c)$ will denote the sign of the linear velocity v_c.*

3 Stabilizing controller

In this section we prove that the control:

$$\omega_e = -4 v_c \left[(\alpha_1\ \alpha_2) y_e + (\alpha_1 + \alpha_2)\sin(\theta_e/2)\ \sigma(v_c)\right] \quad (8)$$

stabilizes system (6). The control design is based on the following change of variables:

$$(x_1, x_2)^T = \left(y_e, \sin\frac{\theta_e}{2}\right)^T \quad (9)$$

With this new state variables, the robot's kinematics represented by system (6) becomes :

$$\begin{pmatrix} \dot{x}_1 \\ \dot{x}_2 \end{pmatrix} = \begin{pmatrix} 0 & 2v_c \cos\frac{\theta_e}{2} \\ 0 & 0 \end{pmatrix} \begin{pmatrix} x_1 \\ x_2 \end{pmatrix} + \begin{pmatrix} 0 \\ \frac{1}{2}\cos\frac{\theta_e}{2} \end{pmatrix} \omega_e \quad (10)$$

For this system, if we look for a feedback control of the type

$$\omega_e = k_1 x_1 + k_2 x_2 \quad (11)$$

such that the poles in closed loop be $-\beta_1$, $-\beta_2$, where $\beta_1, \beta_2 > 0$ and $\beta_1 \neq \beta_2$, we get :

$$\begin{pmatrix} \dot{x}_1 \\ \dot{x}_2 \end{pmatrix} = \begin{pmatrix} 0 & 2v_c \cos\frac{\theta_e}{2} \\ \frac{1}{2}k_1 \cos\frac{\theta_e}{2} & \frac{1}{2}k_2 \cos\frac{\theta_e}{2} \end{pmatrix} \begin{pmatrix} x_1 \\ x_2 \end{pmatrix} \quad (12)$$

where k_1 and k_2 verify:

$$\begin{cases} \beta_1 + \beta_2 &= -\frac{1}{2}k_2 \cos\frac{\theta_e}{2} \\ \beta_1\beta_2 &= -k_1 v_c \cos^2\frac{\theta_e}{2} \end{cases} \quad (13)$$

[1] A velocity profile for v_c is supposed to be given between the initial and final position where $v_c = 0$. When $v_c = 0$, $\omega_c = 0$ as well.

[2] This condition means that the distance to the path is smaller than the reference path curvature radius, ensuring the Frenet frame to be uniquely defined (see [6] for details).

At this stage, as the state matrix and therefore β_1 and β_2 are functions of θ_e, the condition that β_1 and β_2 be strictly positive is not sufficient to guarantee that ω_e stabilizes system (10). Now, let us look for a state transformation $(x_1, x_2)^T = T\ (z_1, z_2)^T$ allowing to get a diagonal equivalent state matrix for system (12). $T = (t_{ij}), 1 \leq i, j \leq 2$ is a constant 2×2 matrix the coefficient of which must verify :

$$\begin{cases} 2v_c \cos\frac{\theta_e}{2}\ t_{21} = -\beta_1\ t_{11} \\ 2v_c \cos\frac{\theta_e}{2}\ t_{22} = -\beta_2\ t_{12} \end{cases} \quad (14)$$

If we suppose $t_{11} \neq 0$ and $t_{12} \neq 0$, by denoting $\alpha_1 = -t_{21}\sigma(v_c)/t_{11}$, and $\alpha_2 = -t_{22}\sigma(v_c)/t_{12}$, we obtain:

$$\beta_1 = 2\alpha_1 v_c \cos\frac{\theta_e}{2}\sigma(v_c)\ ,\ \beta_2 = 2\alpha_2 v_c \cos\frac{\theta_e}{2}\sigma(v_c) \quad (15)$$

Using this notation, the gains are:

$$k_1 = -4\alpha_1\alpha_2 v_c, \text{ and } k_2 = -4(\alpha_1 + \alpha_2)v_c\sigma(v_c) \quad (16)$$

There are several ways to define the matrix T; we consider the particular choice given by :

$$t_{11} = \frac{1}{\alpha_2 - \alpha_1}, \text{ and } t_{12} = -\frac{1}{\alpha_2 - \alpha_1} \quad (17)$$

This choice provides a simple expression for T^{-1}:

$$Z = T^{-1}X = \begin{pmatrix} \alpha_2 & \sigma(v_c) \\ \alpha_1 & \sigma(v_c) \end{pmatrix}\begin{pmatrix} x_1 \\ x_2 \end{pmatrix} \quad (18)$$

considering the state change given by (9), we get

$$z_i = \frac{1}{\alpha_i}\left(\alpha_1\alpha_2\ y_e + \alpha_i\sigma(v_c)\sin\left(\frac{\theta_e}{2}\right)\right), \quad i = 1, 2 \quad (19)$$

and the control (11) becomes:

$$\omega_e = -4v_c\left[(\alpha_1\ \alpha_2)y_e + (\alpha_1 + \alpha_2)\sin(\theta_e/2)\ \sigma(v_c)\right] \quad (20)$$

Using these auxiliary variables z_1 and z_2 we are going to prove that the controller (20) stabilizes the system (6). As $\beta_1 \neq \beta_2$, so long as $|\theta_e| < \pi$, we know from (15) that $\alpha_1 \neq \alpha_2$ and $\alpha_1, \alpha_2 > 0$. The dynamics of z_i, is then :

$$\dot{z}_i = -\alpha_i\ F\ z_i \quad (21)$$

with

$$F = 2\cos\frac{\theta_e}{2}\ |v_c| \quad (22)$$

If we can ensure that the orientation error θ_e remains within $(-\pi, \pi)$, F is ensured to be strictly positive, and therefore both variables z_1 and z_2 verify the condition $z_i\ \dot{z}_i < 0$ as long as $z_i \neq 0$. This condition ensures the exponential convergence of z_1 and z_2 to zero, and as $\alpha_1 \neq \alpha_2$, we deduce from (19) that y_e and θ_e converge also exponentially to the origin. To guarantee the exponential convergence of y_e and θ_e to zero, it suffices to prove that, given any initial configuration $(y_e(0), \theta_e(0)) \in \boldsymbol{R} \times (-\pi, \pi)$, θ_e will not escape from $(-\pi, \pi)$ during the stabilization process. Consider the positive function of z_1 and z_2 :

$$V = \frac{1}{2}\left(z_1^2 + z_2^2\right) \quad (23)$$

In the (x_1, x_2)-plane, the equipotentials of V constitute ellipses centered at the origin (see figure 3). As the derivative of V

$$\dot{V} = -\alpha_1 F z_1^2 - \alpha_2 F z_2^2 \quad (24)$$

is strictly negative, the representative point of the system will never escape out of an ellipse surrounding it at the initial time. To guarantee that $|\theta_e|$ remains strictly smaller than π, we are going to prove that, α_1 and α_2 can be chosen such that, at initial time, the representative point be within the region delimited by an ellipse tangent to both axes $x_2 = -1$ and $x_2 = 1$. To determine the equipotential $V = V_m$ characterizing this tangent ellipse, we compute the maximal value of x_2 on any equipotential of V. Using Lagrange multipliers we get :

$$x_{2max} = -\left(\frac{\alpha_1^2 + \alpha_2^2}{\alpha_1 + \alpha_2}\right)x_1$$

By definition, on the tangent ellipse, $x_{2max} = 1$. The corresponding value of x_1 is:

$$y_e = -\left(\frac{\alpha_1 + \alpha_2}{\alpha_1^2 + \alpha_2^2}\right)$$

The equipotential V_m is then :

$$V_m = \frac{(\alpha_1 - \alpha_2)^2}{\alpha_1^2 + \alpha_2^2} \quad (25)$$

Therefore, if the initial configuration belongs to this ellipse, $|\theta_e|$ will remain smaller than π. Furthermore, for any initial value $y_e(0) \in \boldsymbol{R}$, $\theta_e(0) \in (-\pi, \pi)$, α_1 and α_2 can be chosen such that the representative point be within the equipotential V_m. This last reasoning achieves to prove that control (20) stabilizes exponentially system (6).

4 Control robustness

So far, we have supposed the robot configuration to be exactly known. However, in practice the robot configuration is determined by means of localization techniques, and the measurements obtained are inevitably noisy. As the uncertainties can be estimated and bounded, the robot configuration, with respect to the frame $\mathcal{W}$ is :

$$(\hat{x}_c, \hat{y}_c, \hat{\theta}_c)^T = (x_c + \delta x_c, y_c + \delta y_c, \theta_c + \delta\theta_c)^T \quad (26)$$

with $|\delta x_c| \leq \delta_m x_c$, $|\delta y_c| \leq \delta_m y_c$ and $\delta\theta_c \leq \delta_m\theta_c$. As the position of the fictitious robot P_r is determined by projecting the uncertain robot position on the reference path, one has to consider the noisy value $\hat{P}_r = P_r + \delta P_r$. Using the reasoning introduced in [5] (see figure 2), the expression of δP_r can be deduced by means of simple geometric relations in terms of the reference path curvature radius ρ.

$$\delta P_r = \begin{pmatrix} \delta x_r \\ \delta y_r \\ \delta\theta_r \end{pmatrix} = \begin{pmatrix} \rho\sin\delta\theta_r \\ \rho(1 - \cos\delta\theta_r) \\ \arcsin\left(\frac{\delta x_c}{\rho - y_r}\right) \end{pmatrix} \quad (27)$$

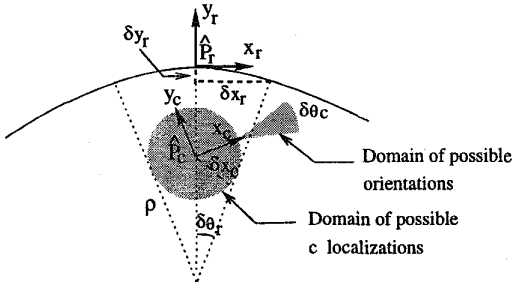

Figure 2: error modeling

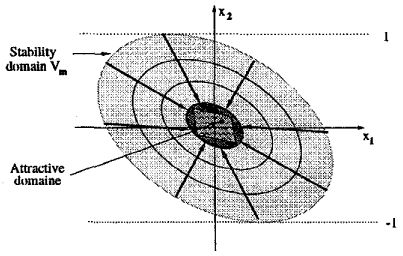

Figure 3: Equipotentials of V, stability and attractive domains in the (x_1, x_2)-plane.

Using these expressions, the error term with respect to $\mathcal{F}$ can be expressed: $\hat{P}_c - \hat{P}_r = \hat{P}_e = P_e + \delta P_e$, where :

$$\delta P_e = \begin{pmatrix} \delta x_e \\ \delta y_e \\ \delta \theta_e \end{pmatrix} = \begin{pmatrix} \cos\hat{\theta}_r \delta x_c + \sin\hat{\theta}_r \delta y_c + y_e \delta\theta_r - \delta x_r \\ -\sin\hat{\theta}_r \delta x_c + \cos\hat{\theta}_r \delta y_c - \delta y_r \\ \delta\theta_c - \delta\theta_r \end{pmatrix} \tag{28}$$

The maximal bounds $\delta_m x_e$, $\delta_m y_e$, and $\delta_m \theta_e$ on $|\delta x_e|$, $|\delta y_e|$ and $|\delta\theta_e|$ can be directly computed from the bounds $\delta_m x_c$, $\delta_m y_c$, and $\delta_m \theta_c$. With this modeling, the question is now: *"Does the control (8) still stabilize system (6) if we consider the noisy measurements $\hat{P}_e = P_e + \delta P_e$ instead of the exact ones?"* As the control loop is fed with uncertain values, it is no more possible to guarantee that y_e and θ_e will converge exactly to zero. However, we are going to prove that control (8) is robust with respect to localization errors, by showing that the representative point of system (6) will converge to a compact attractive domain centered at the origin of the state space. Consider (8) with the noisy values $(\hat{y}_e, \hat{\theta}_e)$:

$$\omega_e = -4v_c[\alpha_1\alpha_2\hat{y}_e + (\alpha_1+\alpha_2)\sin(\frac{\hat{\theta}_e}{2})\sigma(v_c)] \tag{29}$$

As the orientation error is supposed to be small, we can make the first order approximation: $\sin(\hat{\theta}_e/2) \approx \sin(\theta_e/2) + (\delta\theta_e/2)\cos(\theta_e/2)$. Considering control (29), the derivative of z_i is :

$$\dot{z}_i = -\alpha_i F(z_i + \epsilon_i) \tag{30}$$

where

$$\epsilon_i = \frac{1}{\alpha_i}\left(\alpha_1\ \alpha_2\ \delta y_e + (\alpha_1+\alpha_2)\ \frac{\delta\theta_e}{2}\ \cos\left(\frac{\theta_e}{2}\right)\right) \tag{31}$$

Introducing the upper bounds on $|\delta y_e|$ and $|\delta\theta_e|$ coming from the localization procedure, we get:

$$\begin{array}{l} |\epsilon_1| \le \epsilon_{1m} = \alpha_2\ \delta_m y_e + \left(1+\frac{\alpha_2}{\alpha_1}\right)\frac{\delta_m\theta_e}{2} \\ |\epsilon_2| \le \epsilon_{2m} = \alpha_1\ \delta_m y_e + \left(1+\frac{\alpha_1}{\alpha_2}\right)\frac{\delta_m\theta_e}{2} \end{array} \tag{32}$$

Therefore, the convergence condition $z_i\dot{z}_i < 0$, $i = 1, 2$, is guaranteed provided that:

$$|z_i| = \frac{1}{\alpha_i}\ |\alpha_1\ \alpha_2 y_e + \alpha_i\ \sin(\theta_e/2)\ \sigma(v_c)| > \epsilon_{im} \tag{33}$$

In the (x_1, x_2)-space, the equations (33) determine a rhombus centered at the origin. This compact domain constitutes an attractive domain inside which the representative point will converge. A simple upper bound of this domain can be obtained by considering the smallest equipotential of V surrounding it (see figure 3) which is defined by:

$$(\alpha_1 x_1 + x_2)^2 + (\alpha_2 x_1 + x_2)^2 = \epsilon_{1m}^2 + \epsilon_{2m}^2 \tag{34}$$

From this attractive domain one can directly determine a security margin along the reference path, to guarantee obstacle avoidance during the path following process. Indeed, once the system has reached its steady state, the representative point cannot escape from the attractive domain, ensuring the robot to follow closely the path with a small bounded orientation error, in spite of localization errors.

5 Dynamic extension

In this section we present succinctly how the techniques previously developed can be applied to design a robust stabilizing controller for a dynamic extension of the preceding system. So far, the kinematic model we have considered only describes the nonholonomic rolling-without-slipping constraint of the wheels on the floor. A more realistic model would be to consider the linear and angular acceleration as input instead of the velocities:

$$\begin{pmatrix} \dot{x}_c \\ \dot{y}_c \\ \dot{\theta}_c \\ \dot{v}_c \\ \dot{\omega}_c \end{pmatrix} = \begin{pmatrix} \cos(\theta_c)\ v_c \\ \sin(\theta_c)\ v_c \\ \omega_c \\ \tau_{v_c} \\ \tau_{\omega_c} \end{pmatrix} \tag{35}$$

where τ_{v_c} and τ_{ω_c}, respectively stand for the linear and angular accelerations of the robot. With this model, using the same representation as before, the error dynamics can be expressed as follows:

$$\begin{pmatrix} \dot{y}_e \\ \dot{\theta}_e \\ \dot{\eta} \end{pmatrix} = \begin{pmatrix} v_c \sin\theta_e \\ \eta\ F \\ \gamma \end{pmatrix} \tag{36}$$

where $\eta = \frac{\omega_e}{F}$ and F is defined by (22). Here, in addition to y_e and θ_e, the value of $\omega_e = \omega_c - \omega_r$ is supposed to be measured. This value can be deduced from the robot angular velocity ω_c and the reference path curvature $\chi_r = \omega_r/v_r$. Then, if a stabilizing control γ can be determined for system (36), the robot angular acceleration τ_{ω_c} can be expressed as a function of y_e, θ_e, ω_e and $\dot{\chi}_r$ by derivating relation (7). Now, following exactly the same reasoning as before, we can prove that the control :

$$\gamma = -4v_c[\alpha_1\alpha_2\alpha_3 y_e + (\alpha_1\alpha_2 + \alpha_1\alpha_3 + \alpha_2\alpha_3)\sin\tfrac{\theta_e}{2}\sigma(v_c) + (\alpha_1 + \alpha_2 + \alpha_3)\tfrac{\eta}{2}\sigma(v_c)\cos\tfrac{\theta_e}{2}] + v_c\eta^2\sin\tfrac{\theta_e}{2}\sigma(v_c)$$

with $\alpha_1, \alpha_2, \alpha_3 > 0$ and $\alpha_1 \neq \alpha_2 \neq \alpha_3 \neq \alpha_1$ stabilizes exponentially system (36) at the origin. As for the kinematic case, the proof is based on the definition of three auxiliary variables z_1, z_2, and z_3 derived from a transformation similar to the one done in section 3

$$z_i = \alpha_j\alpha_k\sigma(v_c)y_e + (\alpha_j + \alpha_k)\sin\frac{\theta_e}{2} + \frac{\eta}{2}\cos\frac{\theta_e}{2} \qquad (37)$$

with $i \neq j \neq k \neq i$, and $1 \leq i, j, k \leq 3$. As the constant α_i, $i = 1, 2, 3$, are different from each other, if z_1, z_2 and z_3 converge simultaneously to zero, y_e, θ_e, and η will converge to zero as well. As for the kinematic case, the dynamics of z_i is :

$$\dot{z}_i = -\alpha_i F z_i \qquad (38)$$

To prove the convergence of z_i, we need to guarantee that, if the initial value of θ_e is in $(-\pi, \pi)$, the point will never escape from this interval during the stabilization process, ensuring F to remain strictly positive. This can be done by applying the same upper bounding procedure as before, with the help of the positive Lyapunov-like function:

$$V = \frac{1}{2}\left(z_1^2 + z_2^2 + z_3^2\right) \qquad (39)$$

From this, it is possible to prove that this controller is robust with respect to measurement errors by defining an attractive domain around the origin.

6 Experimental results

The proposed control laws have been implemented on one robot of the Hilare family at LAAS-CNRS. The control algorithm has been integrated under the onboard VxWorks real-time system and runs with a sampling time of 25 ms. The robot configuration is obtained from the odometry, which consists in integrating the angular variation of each wheel. A drawback of this classical technique is the accumulation of the error during motion. However, using a probabilistic method, we can estimate and bound these uncertainties. To illustrate the kinematic and dynamic laws, we have conducted two sets of experimentations. The reference paths are composed of line segments and arcs of circle which are the usual outputs of nonholonomic path-planners. Such paths present curvature discontinuities making the control problem harder. In theory, following exactly such a path requires to stop at the discontinuity points. However, when $v_c \neq 0$, the maximal distance value of $|y_e|$ can be expressed as a function of v_c (e.g., $|y_e| < \rho(1-\cos\frac{v_c^2}{2\gamma_{max}\rho^2})$, γ_{max} being the upper bound on the angular acceleration). Provided that y_e remain inside of the stability domain, the robot will move back close to the path as soon as the angular acceleration stops to be saturated. More generally, this raises the problem of velocity and acceleration saturation which is hard to consider in designing the control law. The linear velocity being *an input* of the control, its time profile can be designed in such a way that the linear and angular velocities and accelerations keep away from their upper bound (except at the curvature discontinuities where the angular acceleration is necessarily saturated for $v_c \neq 0$, but, as seen previously, v_c can be adjusted not to escape from the stability domain). This profile depends on the path curvature (one needs to slow down the velocity before turning). In the following experiments we have computed trapezoidal profile for the linear velocity. For comparison purposes, a same profile is used for all the experiments. The characteristics of the robot are: $v_{cmax} = 0.85\ m/s$, $\omega_{cmax} = 0.95\ rad/s$, the maximal linear acceleration is $0.4\ m/s^2$ and the maximal angular acceleration $\gamma_{max} = 1.4\ rad/s^2$. Now, we present the experimental results for the kinematic model and its dynamical extension.

Control using the kinematic law

We present the experiments for two different paths. For both cases we have set $\alpha_1 = 2.0, \alpha_2 = 1.8$. The first path is a U-turn composed of an arc of circle, with a 1 meter radius, connected with two line segments (see figure (4-a)). The reference path and the path executed by the robot are shown on the left, the timeplots of (v_c) and (w_c) are on the right. As it can be predicted, the higher the gains are the faster the system converges. However, with those higher gains the angular acceleration is saturated. The second path corresponds to a lateral movement similar to a parking manoeuvre made of 8 arcs of circle with a large radius (about 6 meters), followed by a sharp turn with a radius of $0.3m$ to get back to the initial position (see figure 5). This experiment shows that the strong discontinuity occurring at the beginning of the sharp turn makes the robot unavoidably deviates locally from the path.

Control for the dynamical extension

The first reference path used for the kinematic case is considered for the dynamic extension (see figure (6-a)). Figure 6 shows the result obtained by fixing $\alpha_1 = 2.0, \alpha_2 = 1.8, \alpha_3 = 2.1$. Comparing the kinematic case (figure (4-a)) with the dynamic one (figure (6-a)), the control law appears clearly smoother in the second case (see the angular velocity profiles at the curvature discontinuity).

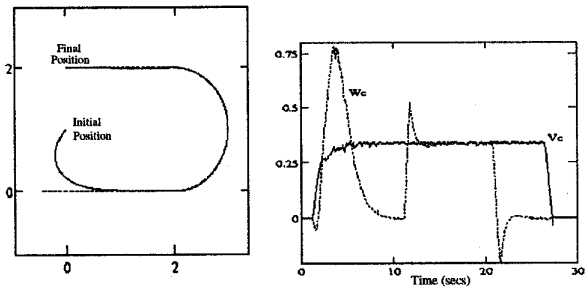

a) The reference and the executed paths

b) Timeplot of the linear and angular velocities

Figure 4: *A U-turn using the kinematic law with* $\alpha_1 = 2.0$ *and* $\alpha_2 = 1.8$.

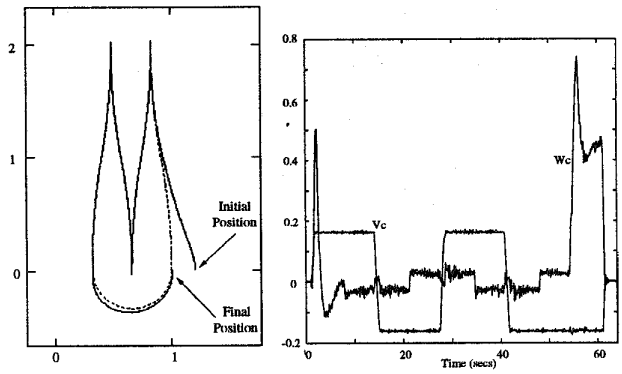

a) The reference and the executed paths

b) Timeplot of the linear and angular velocities

Figure 5: *A parking maneuver followed by a sharp turn using the kinematic law with* $\alpha_1 = 2.0$ *and* $\alpha_2 = 1.8$.

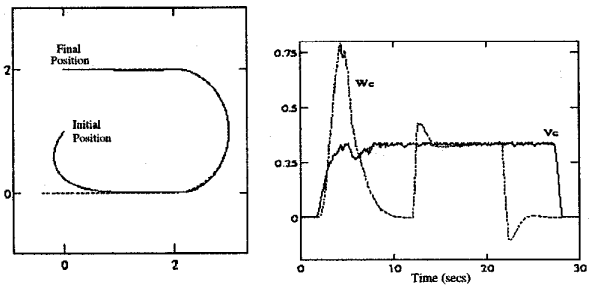

a) The reference and the executed paths

b) Timeplot of the linear and angular velocities

Figure 6: *A U-turn using the dynamic law with* $\alpha_1 = 2.0, \alpha_2 = 1.8$ *and* $\alpha_3 = 2.1$.

7 Conclusion

We have presented a path following controller robust with respect to localization errors, which guarantees a *global and exponential convergence* of the distance and orientation errors with respect to the moving frame. Moreover, *the control parameters can be easily tuned up to find a balance between the convergence velocity and the size of the attractive domain.* This theoretical analysis has been corroborated by real experiments. These experiments show that the proposed laws provide satisfactory results, even when the paths present curvature discontinuities. They also show the interest of considering the dynamic extension which provides smoother velocity profiles than the kinematic law. However, the real implementation has raised the problem of saturating the velocities and the accelerations. There are two different manners to overcome this problem: smoothing the path curvature by using another kind of curves (see for example [3]), or adapting the linear velocity profile to the path shape (in our example, by reducing the linear velocity before the sharp turn).

References

[1] L. Aguilar, T. Hamel, P. Souères "Robust Path Following Control for Wheeled Robots via Sliding Mode Techniques" in Proc. of the *IEEE International Conference on Intelligent Robots and Systems, IROS'97*, Grenoble, France, sept. 1997.

[2] C. Canudas, H.Khennouf, C. Samson, and O.J. Sordalen, "Nonlinear Control Design for Mobile Robots", In *Recent Trends in Mobile Robots.* World Scientific Series in Robotics and Automated Systems, Vol. 11, pp 121–156. , 1993.

[3] S. Fleury, P. Souères, J-P. Laumond, R. Chatila, "Primitives for Smoothing Mobile Robot Trajectories," *IEEE Transaction on Robotics and Automation*, Vol. 11, N° 3, June 1995.

[4] T. Hamel, D. Meizel. "Robust control laws for wheeled mobile robots. In *International Journal of Systems Science* , volume 27, N° 8, pages 695–704, 1996.

[5] T. Hamel, P. Souères, D. Meizel, "A Two-Steps Robust Path-following Controller for Wheeled Robots", In *Proc. of the* 5^{th} *Symposium on Robot Control, SYROCO'97*, Nantes, France, September 1997.

[6] C. Samson, "Path Following and Time-varing Feedback Stabilization of a Wheeled Mobile Robot". In *Proc. of ICARCV'92*, pp RO–13.1.1–13.1.5, Singapore, Septembre 1992.

[7] C. Samson, "Control of Chained Systems. Application to Path Following and Time-Varying Point Stabilization of Mobile Robots," *IEEE Transaction on Automatic Control*, Vol 40, N° 1, Jan. 1995.